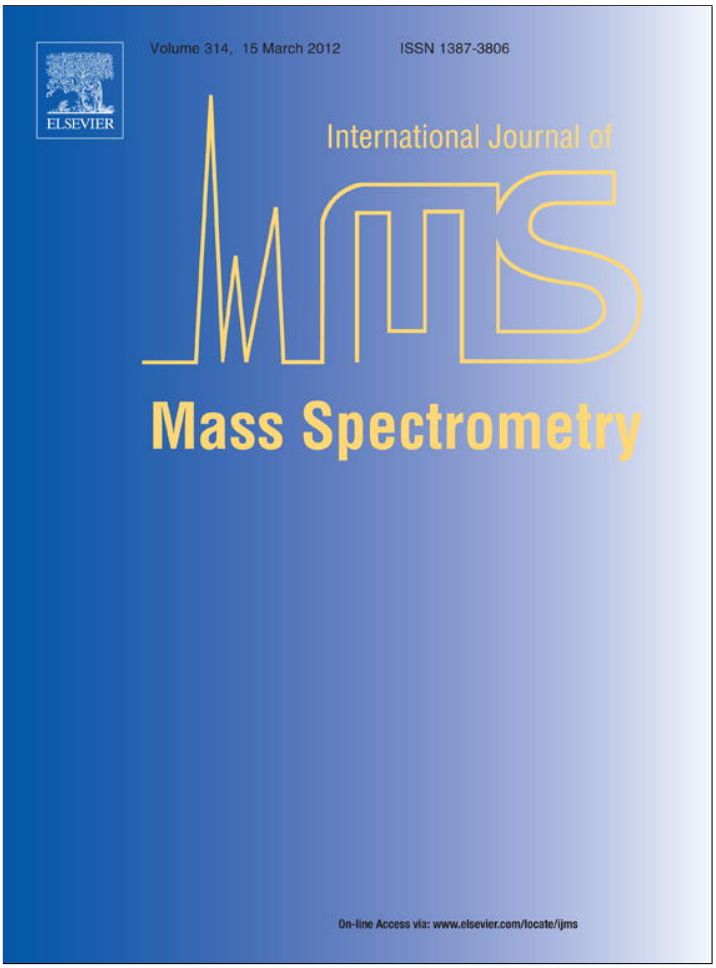

International Journal of Mass Spectrometry 314 (2012) 49–56

Contents lists available at SciVerse ScienceDirect

International Journal of Mass Spectrometry

journal homepage: www.elsevier.com/locate/ijms

Infrared photodissociation of aniline$(H_2O)_n^+$ (n = 7–12) clusters

Md. Alauddin, Jae Kyu Song, Seung Min Park*

Department of Chemistry and Research Center for New Nano Bio Fusion Technology, Kyung Hee University, Seoul 130-701, Republic of Korea

ARTICLE INFO

Article history:
Received 2 November 2011
Received in revised form 2 February 2012
Accepted 8 February 2012
Available online 17 February 2012

Keywords:
Cluster compounds
Infrared spectroscopy
Non-proton transfer process
Hydrogen-bonded topology

ABSTRACT

Infrared (IR) photodissociation spectra of aniline$(H_2O)_n^+$ (n = 7–12) clusters in the region of 2800–3900 cm^{-1} have been explicitly analyzed to elucidate their structures and structural strains in hydrogen bonding networks. Due to the potential barrier between anilide radical and hydrated water clusters (n = 7–12), our experimental and theoretical results suggest that there is no proton-transferred structure in n = 7–12 cluster. The spectroscopic results, combined with DFT calculations show a clear systematic change in hydrogen-bonded topology from a multiple-ring to a cage-like topology as their size increases from n = 7 to 12.

1. Introduction

Van der Waals clusters containing an aromatic compound and solvent molecules permit us to investigate "weak" intermolecular interactions which play a significant role in a great variety of physical, chemical, and biological processes [1–3]. Among many van der Waals cluster systems, hydrated clusters have attracted extensive research interest as hydrogen bonding is certainly the most fundamental interaction of solvation processes in life phenomena [4–6]. Recently, infrared (IR) spectroscopic studies of such clusters in gas phase combined with *ab initio* calculations proved to be highly powerful to provide important information for a clear understanding of geometric structures, intermolecular interactions, conformational dynamics, and proton transfer processes in solvated molecular systems [7–10]. Besides, the branching ratio and mode selectivity in IR predissociation of hydrogen-bonded ternary clusters were examined with an aid of tandem mass spectroscopy [11,12].

Lee and co-workers have extensively studied the infrared spectroscopy of protonated water clusters $H^+(H_2O)_n$ (n = 1–11) in the wavelength region of 2700–3900 cm^{-1} [13–15]. Jordan and co-workers have also investigated the infrared spectroscopy of size-selected protonated water clusters, $H^+(H_2O)_n$ (n = 6–27) through the region of the pronounced "magic number" at n = 21 in the cluster distribution [16]. More recently, Mikami and co-workers reported infrared spectroscopy of protonated water clusters, $H^+(H_2O)_n$ for the clusters ranging from n = 15 to 100 [17]. They found characteristic hydrogen-bonded network for larger closed net structures presumably beyond n = 100 and also observed that the long range influence is significant on the network architecture originating from the nucleation induced by an excess proton.

The infrared spectroscopy of hydrated ions of aromatic molecules has been performed by several groups. Zwier and co-workers has thoroughly studied aromatic cluster compounds such as benzene-$(water)_n$, benzene-$(methanol)_n$, indole-$(water)_n$ clusters and so forth using resonant ion-dip infrared spectroscopy [18–21]. Mikami and co-workers have reported elegant results on benzene-$(water)_1^+$, benzene-$(water)_n^+$ (n = 1–6), benzene-$(water)_n^+$ (n = 1–23) clusters using infrared spectroscopy [22–24]. From the infrared spectra of benzene-$(water)_1^+$ cluster, they concluded that benzene and water molecule formed side structure bound through the charge–dipole interaction. From the IR spectra of benzene-$(water)_n^+$ (n = 2–6), they observed that proton transfer reactions occur from the benzene cation to the water moiety in the larger clusters (n > 3). Nishi and co-workers have performed the IR spectroscopic study of aniline$(H_2O)_n^+$ for small clusters with n = 1–8. With the aid of DFT calculations, they interpreted the spectra for n = 1–5. They found that the most stable structures are branched forms for n = 1–4 clusters, n = 5 cluster turned out to have a stable ring structure; a five-membered ring with the fifth water molecule forming three hydrogen bonds [25].

Here, we report IR spectroscopic study of aniline$(H_2O)_n^+$ (n = 7–12) in the 2800–3900 cm^{-1} region to examine the stable structures of the cluster cations and intra-cluster proton transfer reaction from anilide radical to the water moiety. By comparing the observed spectra with the calculated ones, we have attempted to explain the structural transition from multi-ring to cage-like isomer, which was revealed from a close examination of the free OH

* Corresponding author.
E-mail address: smpark@khu.ac.kr (S.M. Park).

1387-3806/$ – see front matter © 2012 Elsevier B.V. All rights reserved.
doi:10.1016/j.ijms.2012.02.004

Table 1
DFT calculated absolute energy (E, E_{zpve}), relative energy to the most stable isomers (ΔE), and binding energy (E_{bind}) of aniline $(H_2O)_n^+$ (n = 6–12).

Species	E (hartree)	[a] E_{zpve} (hartree)	[b] ΔE (cm^{-1})	[c] E_{bind} (cm^{-1})
Aniline$^+$	−287.353401	−287.236179	0	6568
H_2O	−76.420627	−76.399516	2056	4851
6I	−746.054509	−745.785082	0	4353
6II	−746.040938	−745.775715	1309	5101
7I	−822.498120	−822.204433	0	4065
7II	−822.490289	−822.198470	1927	3447
8I	−898.940537	−898.622470	0	4886
8II	−898.929429	−898.613691	1038	3848
9I	−975.388857	−975.044250	0	4810
9II	−975.381799	−975.039520	320	5130
10I	−1051.836288	−1051.465681	0	7733
10II	−1051.832545	−1051.462409	3407	4326
11I	−1128.299131	−1127.900431	0	5243
11II	−1128.276075	−1127.881637	1315	6558
12I	−1204.748296	1204.323835		
12II	−1204.731688	−1204.311033		

[a] Corrected with zero-point vibrational energies.
[b] Obtained after zero-point vibrational energy correction.
[c] $E_{bind}(n) = -E_{zpve}(n) + E_{zpve}(n-1) + E_{zpve}(H_2O)$, where $E_{zpve}(n-1)$ is the energy of the most stable isomer of the $(n-1)$ ion.

stretching features. Since diverse isomers are possible for medium-sized clusters, we focus our discussion mainly on how the general topologies of the clusters evolve with their sizes.

2. Experimental

The details of the experimental setup were reported previously [11,12,26]. The neutral aniline-water cluster beam was generated by injecting gas mixture of aniline, water, and He at 27 psi into high vacuum through a pulse nozzle (General Valve, Series 9). The gas mixture was obtained by passing He gas over a mixture of aniline and water (aniline:water = 1:5 by volume). Aniline-water clusters were ionized through absorption of two 266 nm photons (the fourth harmonic of a Nd:YAG laser, Continuum, SL III-10) in the ionization stage. The mass selection of hydrated aniline clusters was achieved using a mass gate. The infrared radiation in the range of 2700–4000 cm^{-1} was generated by an IR OPO system consisting of a single Lithium Niobate crystal pumped by a 10 Hz injection seeded Nd:YAG laser (Continuum, SL III-10). Photodissociation action spectra of size-selected hydrated clusters were recorded by monitoring the fragment ion intensities while scanning the IR laser frequency. Density functional theory (DFT) calculations were carried out for the n = 6–12 cluster ions with the *Gaussian 09* program. The calculated total energies of the most stable isomers with zero-point vibration energy (zpve) correction and binding energies of H_2O molecule for them are summarized in Table 1.

3. Results and discussion

3.1. Overview of the IR photodissociation spectra of aniline$(H_2O)_n^+$ (n = 7–12)

Fig. 1 shows infrared photodissociation action spectra of aniline$(H_2O)_n^+$ (n = 7–12) in the region of 2800–3900 cm^{-1}. The dissociation channel chosen for monitoring the spectra is the loss of one water molecule and the intensity of daughter ions so produced is given as a function of the IR wavelength. Mostly, one water ligand was ejected by infrared absorption in our experiment. Although the average total internal energy of the parent ions prior to photodissociation is estimated to be as large as ~0.8 eV and the resultant total internal energy of parent ions after absorption of an infrared photon of ~0.4 eV may exceed the energy required to liberate two water ligands [12], the intensities of daughter ions produced by ejection

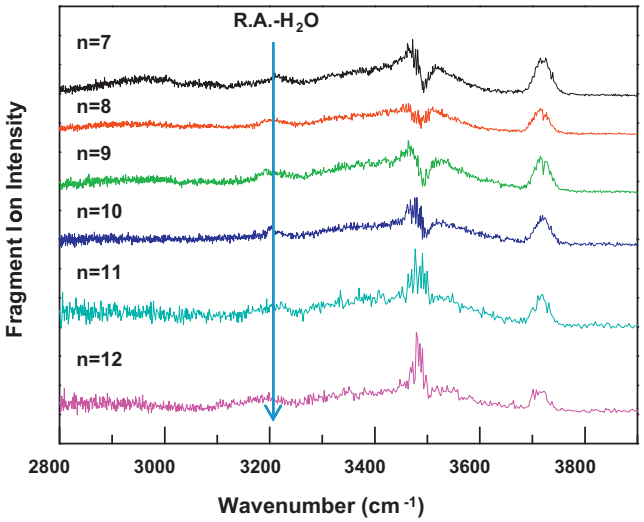

Fig. 1. IR photodissociation action spectra of aniline$(H_2O)_n^+$ (n = 7–12) in the region of 2800–3900 cm^{-1}. The fragment ion monitored for the spectra of aniline$(H_2O)_n^+$ is aniline$(H_2O)_{n-1}^+$ (namely, loss of one water molecule). The IR photodissociation action spectra were corrected by the IR laser power.

of two or more water ligands were not significant. Since we have mass-selected cluster ions, there is no possibility of contamination by other cluster ions. The depletion infrared photodissociation spectra are reproduced in their inverted form in figures for convenience. The IR spectra in Fig. 1 are normalized by the IR laser power and a broad depletion was found around 3486 cm^{-1} is due to the absorption by water involved in the $LiNbO_3$ crystal used for the IR generation.

All the IR spectra show a broader and strong absorption band around 3460 cm^{-1} and a strong OH stretching vibration around 3710 cm^{-1}. The band around 3460 cm^{-1} is assigned to a hydrogen-bonded OH stretching vibration of water moiety. For n = 7–9 clusters, we observed NH stretching vibrations which becomes weaker with the increase in the cluster sizes and disappeared at n = 10 cluster. This indicates that an essential change occurs in the hydrogen-bonded network structure, which is the formation of strong net type structure from the chain structure in water clusters [24].

The most interesting feature of the IR spectra from n = 7 to 12 is that a new absorption band appears near 3200 cm^{-1} in the hydrogen-bonded OH stretching region as shown in Fig. 1 by an arrow. This band can be assigned to the hydrogen-bonded OH stretching vibration of AAD water. A hydrogen bond chain is composed of two co-ordinated water molecules of single acceptor–single donor (AD-water). When one AD water molecule in hydrogen bond chain is bound to another AD water molecule to be transformed to three co-ordinated waters of double donor–single acceptor (ADD) and double acceptor–single donor (AAD), respectively [16,24,27]. Table 2 summarize the observed frequencies of aniline$(H_2O)_n^+$ (n = 7–12) with DFT calculated frequencies and assignments.

3.2. Details of the IR photodissociation spectra of aniline$(H_2O)_n^+$ (n = 7–12)

3.2.1. Aniline$(H_2O)_7^+$

The most stable structure is the isomer **7I** which has a five-membered ring and the fifth and sixth water molecules form three hydrogen bonds with the other water molecules in both sides. The seventh water molecule is bound to the terminal water. The second most stable isomer is **7II** with a six-membered ring, where the sixth and seventh water molecules are bound to two

Table 2
Observed and calculated frequencies (cm^{-1}) and assignments of the infrared spectra of aniline$(H_2O)_n^+$ (n = 7–12).

Species	Observed frequency (cm^{-1})	Isomers	[a]Calculated frequency (cm^{-1})	Assignments
n = 7	~2974	**7I**	2823	Symmetric bonded NH of aniline$^+$
	~3064	**7I**	2895	Anti-symmetric bonded NH of aniline$^+$
	3210	**7I**	3190	Bonded OH of H_2O(AAD)
	~3463	**7I**	3300, 3386, 3444	Bonded OH of H_2O (AD)
	3714	**7I**	3732	Free OH of H_2O (AD)
	3726	**7I**	3744	Anti-symmetric free OH of H_2O(A)
n = 8	~2973	**8I**	2810	Symmetric bonded NH of aniline$^+$
	~3060	**8I**	2851	Anti-symmetric bonded NH of aniline$^+$
	3210	**8I**	3177	Bonded OH of H_2O(AAD)
	~3463	**8I**	3337, 3421, 3568	Bonded OH of H_2O (AD)
	3714	**8I**	3743	Free OH of H_2O (AD) (2C-H_2O)
	3726	**8I**	3755	Anti-symmetric free OH of H_2O(A)
n = 9	3210	**9I**	3161	Bonded OH of H_2O(AAD)
	~3463	**9I**	3265, 3377, 3493, 3563	Bonded OH of H_2O(AD)
	3714	**9I**	3744	Free OH of H_2O (AD)(2C-H_2O)
	3726	**9I**	3756	Anti-symmetric free OH of H_2O(A)
n = 10	3210	**10I**	3131	Bonded OH of H_2O(AAD)
	~3463	**10I**	3339, 3451, 3582	Bonded OH of H_2O(AD)
	3714	**10I**	3745	Free OH of H_2O (AD)(2C-H_2O)
n = 11	3210	**11I**	3181	Bonded OH of H_2O(AAD)
	~3477	**11I**	3481, 3526, 3547	Bonded OH of H_2O(AD)
	3703	**11I**	3736	Free OH of H_2O (3C-H_2O)
	3714	**11I**	3749	Free OH of H_2O (2C-H_2O)
n = 12	3210	**12I**	3172	Bonded OH of H_2O(AAD)
	~3477	**12I**	3463, 3494, 3523	Bonded OH of H_2O(AD)
	3703	**12I**	3734	Free OH of H_2O (3C-H_2O)
	3714	**12I**	3748	Free OH of H_2O (2C-H_2O)

2C, two co-ordinate; 3C, three co-ordinate; A, acceptor; AD, single acceptor–single donor; AAD, double acceptor–single donor.
[a] Calculated using B3LYP/cc-pVDZ level of theory. Calculated values were corrected by multiplying the frequency factor, f = 0.981.

terminal waters. The DFT calculated optimized structure for isomer **7I** and **7II** are shown in Fig. 6. The infrared photodissociation spectrum of aniline$(H_2O)_7^+$ and calculated spectra of isomers **7I** and **7II** are shown in Fig. 2(a). The observed spectrum shows three strong absorption bands at ~3463, 3714, 3726 cm^{-1} and three weak bands at ~2974, ~3064, 3210 cm^{-1}. It is gratifying that the calculated spectrum of the isomer **7I** agrees well with the observed spectrum. We have assigned the absorption bands at ~2974, ~3064,

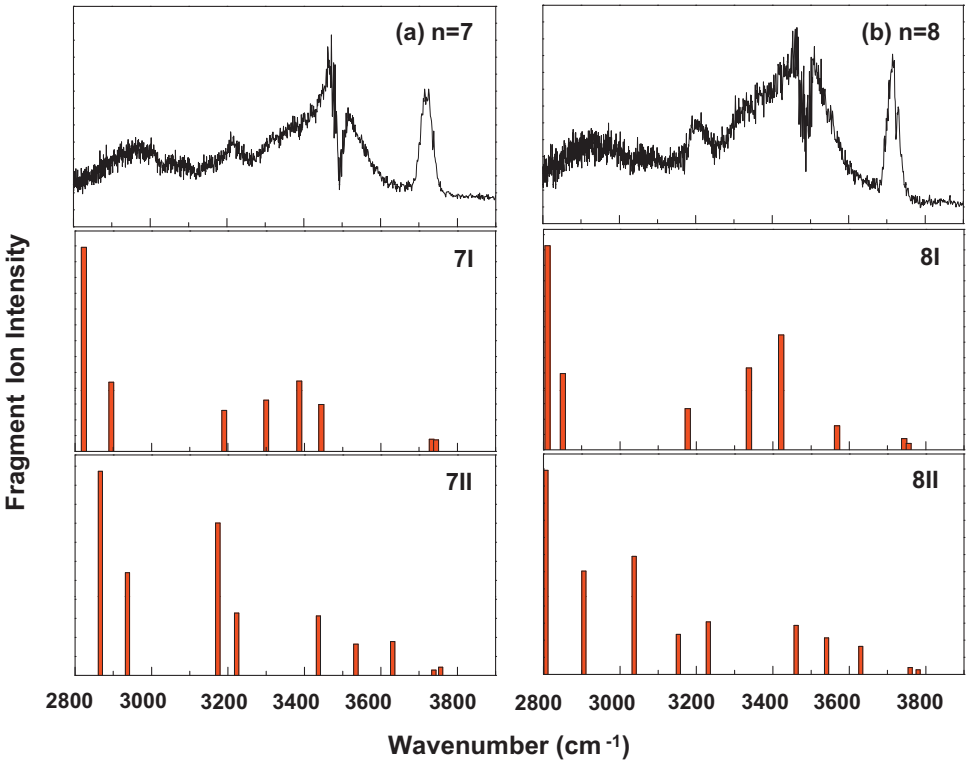

Fig. 2. IR photodissociation action spectra of (a) aniline$(H_2O)_7^+$ and (b) aniline$(H_2O)_8^+$ and their calculated spectra for the two most stable isomers **I** and **II**.

3210, ~3463, 3714 and 3726 cm^{-1} to the symmetric bonded NH of aniline$^+$, anti-symmetric bonded NH of aniline$^+$, hydrogen-bonded OH of H_2O (AAD water), hydrogen-bonded OH of H_2O (AD water), free OH of H_2O (AD water), and anti-symmetric free OH of H_2O (A), respectively. Isomer **7II** is less stable by 1309 cm^{-1} than isomer **7I** and the calculated spectrum for isomer **7II** is not coincident with the observed spectrum. Therefore, we propose that the dominant form of aniline$(H_2O)_7^+$ is isomer **7I**. But the relative intensity of the free OH vibration of H_2O is not in good agreement between the experimental and calculated result, presumably due to the weaker hydrogen bonding network in the water clusters where the strong hydrogen bonding network weakens the strength of the dangling OH vibration. As the spectral resolution in the free OH region is not enough, we deconvoluted the spectra into Lorentzian components for n = 7–12 clusters which is shown in Fig. 5.

An intriguing feature of the spectrum of aniline$(H_2O)_7^+$ is that the intensity of the bonded NH stretching vibrations are weak and also their bandwidths are broader. These results indicate that the intermolecular hydrogen bonding becomes stronger with the increase in cluster sizes [28]. According to the result of vibrational frequency calculation of the isomer **7I**, the symmetric NH stretching around 2823 cm^{-1} is coupled with the CH stretching vibrations which shifted NH vibrations towards lower frequency region.

3.2.2. Aniline$(H_2O)_8^+$

The infrared photodissociation spectrum of aniline$(H_2O)_8^+$ and calculated spectra of isomers **8I** and **8II** are shown in Fig. 2(b). The most stable structure is the isomer **8I** and the second most stable isomer is **8II** as shown in Fig. 6 and the energy difference between the two is shown in Table 1.

The observed spectrum shows four strong absorption bands at 3210, ~3463, 3714, and 3726 cm^{-1} and two very weak bands at ~2973 and ~3060 cm^{-1}. The relative positions of the calculated spectrum of isomer **8I** strongly support the observed one. We have assigned the absorption bands at ~2973, ~3060, 3210, ~3463, 3714 and 3726 cm^{-1} to the symmetric bonded NH of aniline$^+$, anti-symmetric bonded NH of aniline$^+$, hydrogen-bonded OH of H_2O (AAD water), hydrogen-bonded OH of H_2O (AD water), free OH of H_2O (AD) (two co-ordinate H_2O molecule), and anti-symmetric free OH of H_2O (A), respectively. The most important feature is that the intensity of the hydrogen-bonded OH stretching vibration of AAD water increases with the increase in cluster sizes, whereas NH absorption bands are broad and very weak. This reflects a stronger hydrogen-bonding network.

3.2.3. Aniline$(H_2O)_9^+$

The optimized structure for isomer **9I** and **9II** are shown in Fig. 6 and the energy difference between **I** and **II** clusters is listed in Table 1. Fig. 3(a) shows the infrared photodissociation spectrum of aniline$(H_2O)_9^+$ and calculated spectra of the isomers **9I** and **9II**. The observed spectrum shows four strong absorption bands at 3210, ~3463, 3714, 3726 cm^{-1}. Consequently, a very weak and broad absorption band is observed in NH stretching region which implies very strong hydrogen-bonding network among water molecules. According to the result of vibrational frequency calculation of the isomer **9I** and **9II**, one stick spectrum is observed around 2875 cm^{-1} which is for the symmetric NH stretching vibration. On the other hand, the intensity of NH stretching band is very large due to the strongly coupled with CH stretching vibrations. The co-existence of isomers **9I** and **9II** are not impossible as the energy differences between **9I** and **9II** is 1038 cm^{-1}, according to the DFT calculations (Table 1). We have assigned the absorption bands at 3210, ~3463, 3714 and 3726 cm^{-1} to the hydrogen-bonded OH of H_2O (AAD water), hydrogen-bonded OH of H_2O (AD water), free OH of H_2O (AD) (two co-ordinate H_2O molecule), and anti-symmetric free OH of H_2O (A), respectively. But the relative intensity of the free OH vibration of H_2O is not quite satisfactory between the experimental and calculated one. The observed absorption band is very strong compared to the calculated one. This result may stem from the weaker hydrogen-bonding network in the water clusters because strong hydrogen-bonding network weakens the strength of the dangling OH vibration. For clear explanation, we deconvoluted the spectra into Lorentzian components in the free OH region for n = 7–12 clusters which is shown in Fig. 5.

As the number of water molecules increased with the increase in cluster size, hydrogen-bonded network became stronger and the intensity around the absorption band at 3200 cm^{-1} increased.

3.2.4. Aniline$(H_2O)_{10}^+$

From n = 10 cluster, we found that the cluster has a great tendency to form a three co-ordinate structure. The most stable isomer of n = 10 is **10I** and the second most stable isomer is **10II** as shown in Fig. 6. The infrared photodissociation spectrum of aniline$(H_2O)_{10}^+$ and calculated spectra of the isomers **10I** and **10II** are illustrated in Fig. 3(b). The observed spectrum shows three strong absorption bands at 3210, ~3463, and 3714 cm^{-1} which are assigned to the hydrogen-bonded OH of H_2O (AAD water), hydrogen-bonded OH of H_2O (AD water), free OH of H_2O (AD) (two co-ordinate H_2O molecule), respectively. On the other hand, we have not observed anti-symmetric OH stretching vibration of H_2O and our calculated spectra for **10I** and **10II** isomers strongly support this behavior. We cannot neglect the contribution of **10I** isomer as the energy differences between **10I** and **10II** is 320 cm^{-1} which is very small, according to the DFT calculations (Table 1). This indicates that the water molecules located at the end of water chain become closer to one another via strong hydrogen-bonding.

3.2.5. Aniline$(H_2O)_{11}^+$

The most stable isomer of n = 11 is **11I** and the second most stable isomer is **11II** as depicted in Fig. 6. The infrared photodissociation spectrum of aniline$(H_2O)_{11}^+$ and calculated spectra of the isomers **11I** and **11II** are shown in Fig. 4(a). The calculated spectrum of the isomer **11I** agrees well with the observed spectrum. We observed four absorption bands at 3210, ~3477, 3703, and 3714 cm^{-1} which are assigned to the hydrogen-bonded OH of H_2O (AAD water), hydrogen-bonded OH of H_2O (AD water), free OH of H_2O (AD) (three co-ordinate H_2O molecule), and free OH of H_2O (AD) (two co-ordinate H_2O molecule), respectively.

The most interesting feature is that the two co-ordinate free OH vibration of H_2O molecules split into two spectra. One is three co-ordinates free OH of H_2O which has absorption band at 3703 cm^{-1} and the other is two co-ordinates free OH of H_2O whose absorption band appears at 3714 cm^{-1}. On the contrary, the intensity of free OH stretching vibration decreased compared to the n = 9, 10 clusters, which indicates that a strong three co-ordinated structure are formed via hydrogen bonding among the water molecules. For clear explanation, we deconvoluted the spectra into Lorentzian components in the free OH region for n = 7–12 clusters which is shown in Fig. 5.

3.2.6. Aniline$(H_2O)_{12}^+$

The infrared photodissociation spectrum of aniline$(H_2O)_{12}^+$ and calculated spectra of the isomers **12I** and **12II** are shown in Fig. 4(b). The observed spectrum shows four strong absorption bands at 3210, ~3477, 3703, and 3714 cm^{-1} which are assigned to the hydrogen-bonded OH of H_2O (AAD water), hydrogen-bonded OH of H_2O (AD water), and free OH of H_2O (AD) (three co-ordinate H_2O molecule), and free OH of H_2O (AD) (two co-ordinate H_2O molecule), respectively. It is of note that the intensity of the three-coordinated free OH of H_2O (3703 cm^{-1}) is stronger than that of the two-coordinated free OH of H_2O (3714 cm^{-1}) which

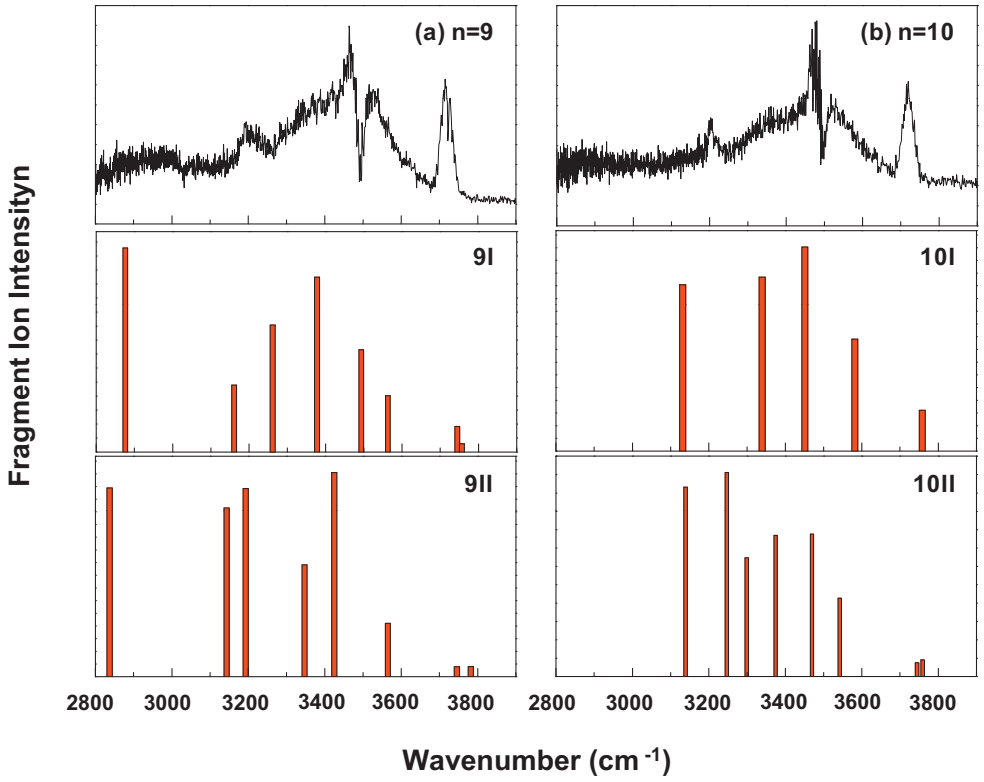

Fig. 3. IR photodissociation action spectra of (a) aniline$(H_2O)_9^+$ and (b) aniline$(H_2O)_{10}^+$ and their calculated spectra for the two most stable isomers **I** and **II**.

indicates that a "real" cage-like structure evolved from a multi-ring structure. Weak free OH vibration is expected when the surrounding hydrogen bonds are stronger because the electron density on the free OH bond is slightly withdrawn by the neighboring proton donor molecules. The free OH vibration of three coordinated H_2O molecule shows that the hydrogen bonds increase their mean strengths as the network grows. The optimized structures of $n = 12$ cluster (isomers **12I** and **12II**) in Fig. 6 have a structure

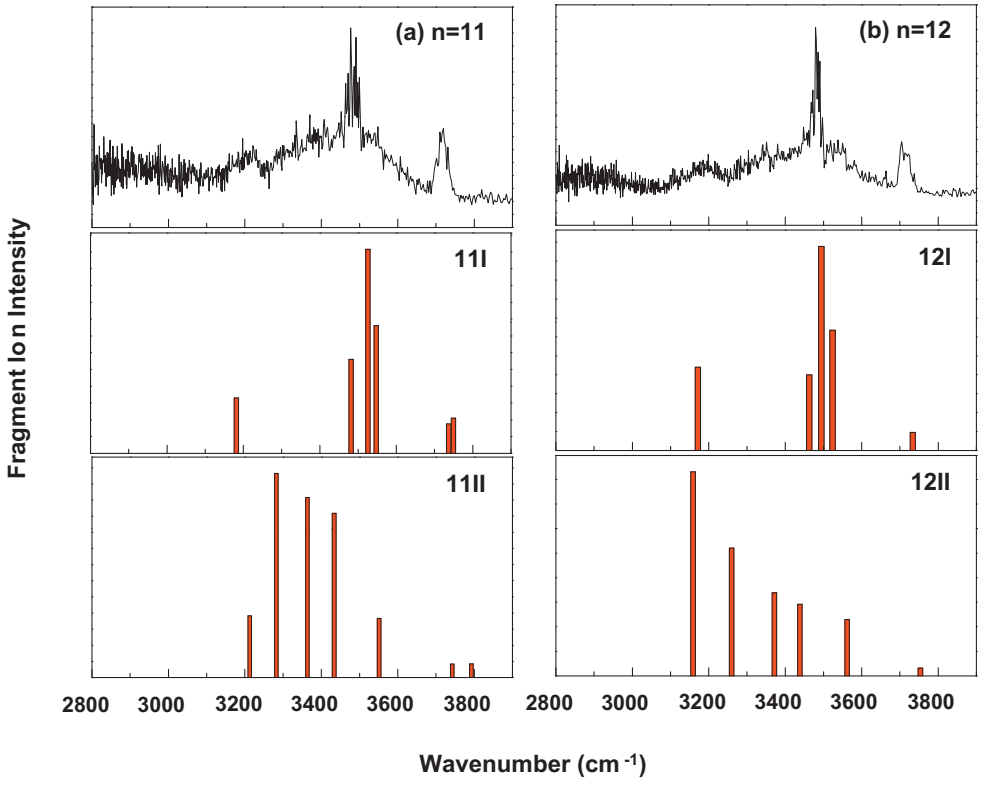

Fig. 4. IR photodissociation action spectra of (a) aniline$(H_2O)_{11}^+$ and (b) aniline$(H_2O)_{12}^+$ and their calculated spectra for the two most stable isomers **I** and **II**.

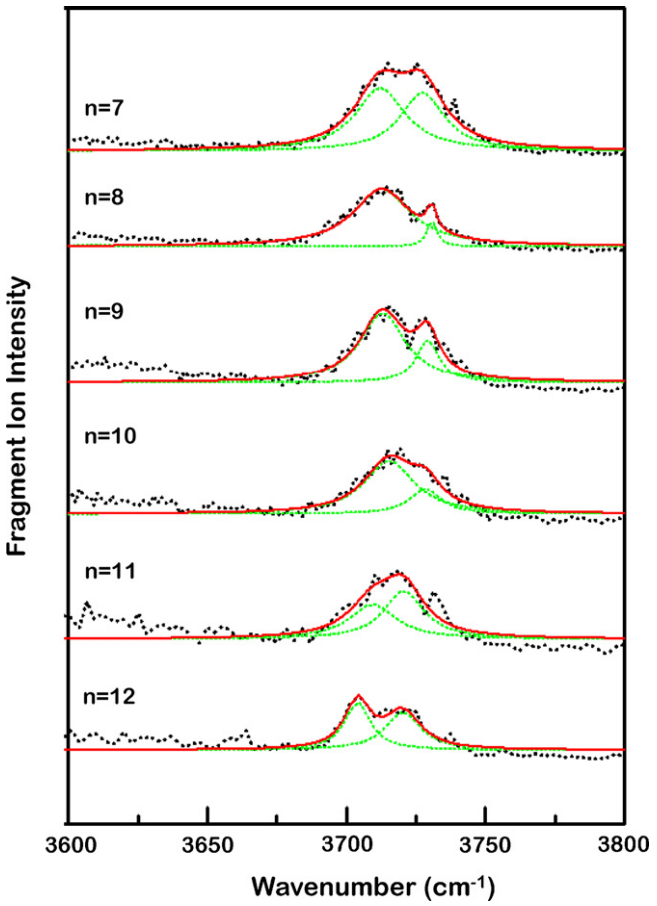

Fig. 5. Enlarged view of the IR photodissociation action spectra of aniline$(H_2O)_n^+$ (n = 7–12) in the region of 3600–3800 cm^{-1}. The observed spectra (shown by dots) are decomposed into Lorentzian components (dotted curves). Solid curves represent the sum of the Lorentzian components.

of cage-like shape (specially for isomer **12I**), which strongly supports our observed spectrum.

3.3. Non proton-transferred form

In the infrared photodissociation spectra for n = 7–9 clusters, we observed a broad absorption band around 3460 cm^{-1} in addition to NH stretching vibrations. We also observed hydrogen-bonded OH stretching vibration near 3200 cm^{-1} which became stronger with the increase in cluster sizes. It has been already explained that the broad absorption band around 3460 cm^{-1} is responsible for proton-transferred structure with the ring of hydrogen-bonding network [25]. Nishi and co-workers suggested that the n = 6–8 cluster ions have a proton-transferred structures, where the proton of the NH bond is transferred to the water moiety, as they showed broad absorption band around 3400 cm^{-1} [25]. However, they could not observe any absorption bands in the NH stretching region for n = 6–8 clusters and they did not show any calculated structures for n = 6–8 clusters. Kleinermanns and co-workers showed that the phenol$(H_2O)_m^+$ clusters with m = 4, 7, and 8 have the proton-transferred form which displays a very broad absorption band around 3430 cm^{-1} [29]. On the other hand, we also observed a broad absorption band around 3460 cm^{-1} along with NH stretching vibrations. It is well-known that proton-transfer occurs with no barrier, or with an extremely small barrier height. In our experiment, the hydrogen-bonded NH stretching vibrations for n = 7–9 clusters were barely observable, which suggests that proton-transfer has not occurred and the potential barrier between the two local minima, $C_6H_7N^+$–$(H_2O)_n$ and C_6H_6N–$H^+(H_2O)_n$ along the reaction co-ordinate was quite low for n = 7–9 clusters. The chromophore switching is solely determined by a difference in proton affinity between the anilide radical and the solvent molecules [30]. For larger clusters, the hydrogen-bonded NH stretching vibrations disappeared. This implies that proton affinity of anilide radical is similar to that of the hydrogen-bonded water clusters. On the contrary, the calculated structures for isomers **9I**, **10I**, **11I** and **12I** do not show any proton-transferred structures and they are still $C_6H_7N^+$–$(H_2O)_n$. Although we did not observe NH stretching vibrations for n = 10–12 clusters, there seems to be a certain potential barrier between the anilide radical and water clusters which is a burden to complete proton transfer.

The basicity of $(H_2O)_n$ clusters increases with the number of water molecules there-in. The proton affinity of anilide radical is 215.6 kcal/mol [31] and the proton affinities of $(H_2O)_1$, $(H_2O)_2$, $(H_2O)_3$, $(H_2O)_4$, $(H_2O)_5$, and $(H_2O)_6$ clusters in gas-phase are 167, 195, 206, 215, 216 and 217 kcal/mol, respectively and they increased by very small amount with the increase of water molecules [32]. In case of aniline$(H_2O)_n^+$ (n = 7–9) clusters, the NH stretching vibrations give broad bandwidths and the intensities are very low and n = 10–12 clusters have no NH stretching vibrations. Since the proton affinities of $(H_2O)_{4-6}$ or larger clusters are not larger than that of anilide radical, water clusters cannot pull out a proton from anilide radical to water clusters. Consequently, we have not obtained any stable structures by DFT calculations where a proton is transferred from anilide radical to water moiety for n = 7–12 clusters. Henceforth, we suggest that proton transfer does not occur from anilide radical to water moiety for n = 7–12 cluster.

3.4. Hydrogen-bonded topologies of aniline$(H_2O)_n^+$ (n = 7–12) clusters

The free OH stretching vibration of H_2O molecules is highly important to explain the hydrogen-bonded topologies. For n = 7 cluster, we observed two OH stretching vibrations: one is the free OH stretching vibration for two co-ordinated H_2O molecule (AD) at 3714 cm^{-1} and the other is the anti-symmetric free OH vibration of H_2O (A) at 3726 cm^{-1}. Although two OH stretching vibrational bands are not reproduced very well in the IR spectra, the DFT calculation strongly suggests this assignment. With the increase in cluster size from n = 7 to 9, the intensity of anti-symmetric free OH vibration of H_2O (A) at 3726 cm^{-1} decreased and finally disappeared at n = 10 cluster. On the contrary, a new absorption band appeared at 3703 cm^{-1} (free OH vibration of three co-ordinated H_2O molecules) along with 3714 cm^{-1} band and with the increase in cluster size (n = 12), three co-ordinated free OH of H_2O (3703 cm^{-1}) band became stronger. This suggests that water molecules at the end of the water chain became closer to one another via strong hydrogen bonding from the multi-ring structure and ultimately it would form a complete cage-like structure with the increase of cluster sizes. It has been already proved that water cage formation is completed at the same size (n = 21) in both the benzene–water cluster cations and protonated water clusters [24]. Although chromophores (aniline, benzene) are totally different, the spectral behaviors of their hydrated clusters are quiet similar to us in the OH vibrational region. However, for n = 12, the intensity of the two co-ordinated free OH of H_2O band decreased, which reflects that the electron density is slightly withdrawn from the free OH bond by the neighboring proton donor molecules. The DFT calculated structure for n = **9I**, **10I**, **11I**, and **12I** isomers (Fig. 6) also support the change of the hydrogen-bonded topologies.

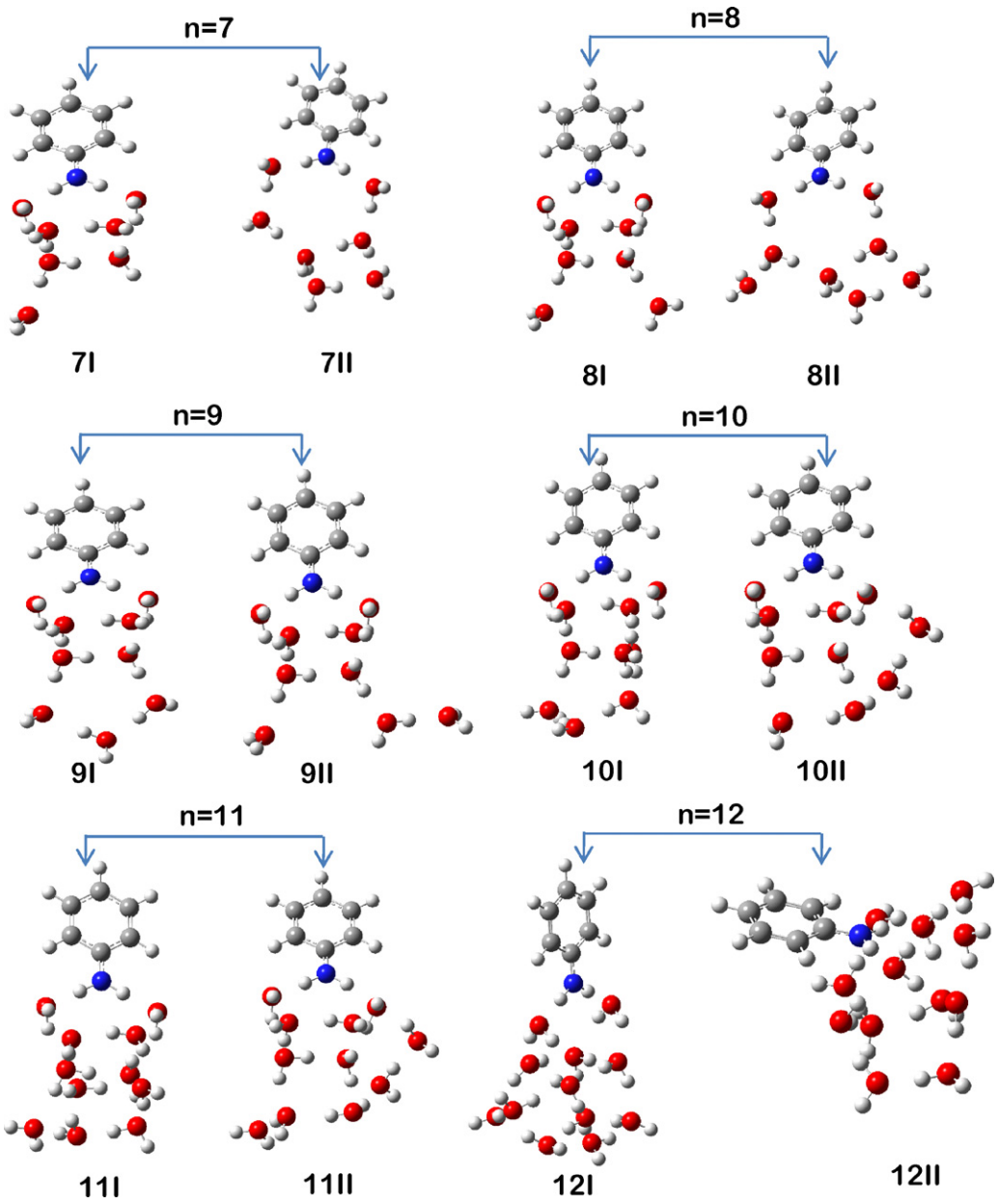

Fig. 6. The optimized structures of aniline$(H_2O)_n^+$ (n = 7–12) at the B3LYP/cc-pVDZ level of theory.

4. Conclusion

Size-selected aniline$(H_2O)_n^+$ (n = 7–12) clusters were prepared and their IR photodissociation spectra were obtained in the region of 2800–3900 cm^{-1}. Also, the geometry optimization and the vibrational frequency evaluation were carried out at the B3LYP/cc-pVDZ level of theory to elucidate their structures. For all the cluster cases, a broad absorption band was found around at 3460 cm^{-1} which is assigned to the hydrogen-bonded OH of H_2O (AD) molecules. Due to a potential barrier between the anilide radical and water clusters, our experimental and theoretical results lead us to conclude that proton-transfer does not occur from n = 7 to 12 cluster. Besides, from the close observation of the experimental and theoretical results in the free OH region, it is apparent that the structure of cluster ions evolves from a multi ring-like topology to a cage-like topology as their size increases from n = 7 to 12.

Acknowledgement

This work was supported by the National Research Foundation of Korea (No. 2009-0079060).

References

[1] E.J. Bieske, J.P. Maier, Chem. Rev. 93 (1993) 2603–2621.
[2] B. Brutschy, Chem. Rev. 100 (2000) 3891–3920.
[3] T.S. Zwier, Ann. Rev. Phys. Chem. 47 (1996) 205–241.
[4] X. Qu, J.B. Chaires, J. Am. Chem. Soc. 121 (1999) 2649–2650.
[5] S. Nonose, S. Iwaoka, K. Mori, Y. Shibata, K. Fuke, Eur. Phys. J. D 34 (2005) 315–319.
[6] H. Saigusa, S.H. Urashima, H. Asami, J. Phys. Chem. A 113 (2009) 3455–3462.
[7] T.S. Zwier, J. Phys. Chem. A 105 (2001) 8827–8839.
[8] K. Mizuse, T. Hamashima, A. Fujii, J. Phys. Chem. A 113 (2009) 12134–12141.
[9] S.H. Urashima, H. Asami, M. Ohba, H. Saigusa, J. Phys. Chem. A 114 (2010) 11231–11237.
[10] S. Enomoto, M. Miyazaki, A. Fujii, N. Mikami, J. Phys. Chem. A 109 (2005) 9471–9480.

[11] Md. Alauddin, J.K. Song, S.M. Park, Chem. Phys. Lett. 498 (2010) 14–17.
[12] Md. Alauddin, J.K. Song, S.M. Park, Chem. Phys. Lett. 506 (2011) 156–160.
[13] C.K. Lin, C.C. Wu, Y.S. Wang, Y.T. Lee, H.C. Chang, J.L. Kuo, M.L. Klein, Phys. Chem. Chem. Phys. 7 (2005) 938–944.
[14] J.C. Jiang, Y.S. Wang, H.C. Chang, S.H. Lin, Y.T. Lee, G.N. Schatterburg, H.C. Chang, J. Am. Chem. Soc. 122 (2000) 1398–1410.
[15] L.I. Yeh, M. Okumura, J.D. Myers, J.M. Price, Y.T. Lee, J. Chem. Phys. 91 (1989) 7319–7330.
[16] J.W. Shin, N.I. Hammer, E.G. Diken, M.A. Johnson, R.S. Walters, T.D. Jaeger, M.A. Duncan, R.A. Christie, K.D. Jordan, Science 304 (2004) 1137–1140.
[17] K. Mizuse, A. Fujii, N. Mikami, J. Chem. Phys. 126 (2007) 231101–231104.
[18] C.J. Gruenloh, J.R. Carney, C.A. Arrington, T.S. Zwier, S.Y. Fredericks, K.D. Jordan, Science 276 (1997) 1678–1681.
[19] C.J. Gruenloh, J.R. Carney, F.C. Hagemeister, C.A. Arrington, T.S. Zwier, S.Y. Fredericks, J.T. Wood III, K.D. Jordan, J. Chem. Phys. 109 (1998) 6601–6614.
[20] R.N. Pribble, F.C. Hagemeister, T.S. Zwier, J. Chem. Phys. 106 (1997) 2145–2157.
[21] J.R. Carney, F.C. Hagemeister, T.S. Zwier, J. Chem. Phys. 108 (1998) 3379–3382.
[22] M. Miyazaki, A. Fujii, T. Ebata, N. Mikami, Chem. Phys. Lett. 349 (2001) 431–436.
[23] M. Miyazaki, A. Fujii, T. Ebata, N. Mikami, Phys. Chem. Chem. Phys. 5 (2003) 1137–1148.
[24] M. Miyazaki, A. Fujii, T. Ebata, N. Mikami, J. Phys. Chem. A 108 (2004) 10656–10660.
[25] Y. Inokuchi, K. Ohashi, Y. Honkawa, N. Yamamoto, H. Sekiya, N. Nishi, J. Phys. Chem. A 107 (2003) 4230–4237.
[26] S.H. Nam, H.S. Park, M.A. Lee, N.R. Cheong, J.K. Song, S.M. Park, J. Chem. Phys. 126 (2007) 224302–224309.
[27] U. Buck, I. Ettischer, M. Melzer, V. Buch, J. Sadlej, Phys. Rev. Lett. 80 (1998) 2578–2581.
[28] Y. Inokuchi, K. Ohashi, Y. Honkawa, H. Sekiya, N. Nishi, Chem. Phys. Lett. 359 (2002) 283–288.
[29] K. Kleinermanns, C. Janzen, D. Spangenberg, M. Gerhards, J. Phys. Chem. A 103 (1999) 5232–5239.
[30] S. Sato, N. Mikami, J. Phys. Chem. 100 (1996) 4765–4769.
[31] N. Russo, M. Toscano, A. Grand, T. Mineva, J. Phys. Chem. A 104 (2000) 4017–4021.
[32] R. Knochenmuss, O. Cheshnovsky, S. Leutwyler, Chem. Phys. Lett. 144 (1988) 317–321.